Original Research Article

Examining the Poisoning Effects of SO_2, CO_2, and NO_2 Contaminants on Pt and Ru Catalysts in Ammonia Decomposition Reactions

Michael Sulla

Santa Susana High School, 3570 E. Cochran St., Simi Valley, CA, 93063, United States

ABSTRACT

Ammonia (NH_3) is a promising candidate for molecular hydrogen storage. To release hydrogen, ammonia must be decomposed in a catalytic decomposition reaction, which often utilizes Ruthenium (Ru) -based catalysts. However, Ru is vulnerable to poisoning from contaminants like Nitrogen Dioxide (NO_2), Carbon Dioxide (CO_2), and Sulfur Dioxide (SO_2), which are often present within ammonia streams. Through the use of density functional theory (DFT) simulations, the adsorption of NO_2, CO_2, SO_2, and NH_3 was modeled interacting with Ru and Platinum (Pt) catalyst surfaces. These simulations revealed that Pt is highly vulnerable to NO_2 and SO_2 poisoning, while exhibiting unfavorable interactions with NH_3. As such, our results suggest that Pt is unsuitable as a catalyst for an NH_3 decomposition reaction. However, it may still be used as a component to filter NO_2 and SO_2 contaminants. Ru also exhibits SO_2 and NO_2 binding modes, but these interactions are comparatively weaker than the Pt surface interactions. In contrast to the Pt surface, the Ru surface did show favorable binding modes with NH_3. Overall, these results confirm that Ru-based catalysts are more suitable than Pt-based catalysts for ammonia decomposition, but are still vulnerable, particularly to NO_2 and SO_2 contaminants.

Keywords: Catalysis; Computational Chemistry; Surface Chemistry; DFT; Ammonia

INTRODUCTION

In recent years, more attention has been turned towards the use of hydrogen (H_2) as a fuel source (1). This is due to its high energy density, sustainable production and low environmental impact; its combustion produces no carbon emissions (2). However, hydrogen fuel exhibits several drawbacks, primarily its relatively low density, and thus its challenging storage (3). Ammonia (NH_3) is a promising candidate to address this issue. Ammonia can be decomposed into hydrogen and has approximately twice the volumetric energy density of H_2, making it a promising option for H_2 storage (4). However, ammonia decomposition is thermodynamically unfavorable, requiring a catalyst. Ruthenium (Ru) is one of the preferred catalysts for this process (5). The net reaction for an ammonia decomposition reaction catalyzed by Ru is $NH_3(g) \rightarrow N_2(g) + H_2(g)$, with $\Delta H = +46$ kJ/mol. NH_3 is first adsorbed onto the Ru surface, where it undergoes dissociation reactions. This

Corresponding author: Michael Sulla, E-mail: m.sulla343@gmail.com.

Accepted August 4, 2026
https://doi.org/10.70251/HYJR2348.44671675

dissociation forms intermediaries NH_2 and NH, which quickly dissociate into individual nitrogen and hydrogen atoms. The individual atoms quickly recombine to form nitrogen (N_2) and H_2 before desorbing from the surface (6). However, many factors can affect the efficiency of a Ru catalyst. Poisoning by oxygen-containing compounds, which disrupt active sites, is of particular importance in ammonia decomposition reactions (7). Oxygen-containing compounds, including sulfur dioxide (SO_2), nitrogen dioxide (NO_2), and carbon dioxide (CO_2), often contaminate ammonia streams, including ammonia derived from combustion, though prevalence varies by production route (8).

As such, this study aims to evaluate the vulnerability of Ru and Platinum (Pt) catalysts to poisoning by SO_2, NO_2, and CO_2 using Density Functional Theory (DFT) simulations. By comparing the adsorption behavior of ammonia and these contaminants on both Pt and Ru, this work seeks to determine the relative susceptibility of Ru to poisoning when compared to other Pt group metals and thus its relative suitability as a catalyst for ammonia decomposition reactions. Previous work has shown that Pt group metals are vulnerable to poisoning by oxygen containing compounds: with platinum noted as being particularly vulnerable (9). Additionally, Larghi *et al*. have demonstrated that Ru is vulnerable to poisoning from sulfur-containing compounds in particular (10). Therefore, it is postulated that Ru will be less vulnerable to NO_2 and CO_2 poisoning than Pt, but still vulnerable to SO_2.

METHODS AND MATERIALS

The primary tool utilized for analysis is Quantum ESPRESSO (11, 12), a DFT tool, which was accessed via NanoHub.org, an open-source hub for computational modeling tools. DFT is a common computational chemistry approach used to model quantum systems by approximating solutions to the Schrödinger Equation. This modeling technique maps the probable density of the electron clouds of all the atoms in a system and uses these predictions to model the Hamiltonian operator of the system. Through this, the material properties can be determined (13). These properties were used to generate and analyze an adsorption energy versus distance graph. Through the analysis of these graphs, chemisorption and physisorption points and energies can be determined (14).

All simulations were performed using Quantum ESPRESSO version 6.3 with the Perdew-Burke-Ernzerhof (PBE) generalized gradient approximation as the exchange-correlation functional. Norm-conserving pseudopotentials were employed, with the FHI98PP pseudopotential set used for all constituent elements (Pt, Ru, N, H, O, C, and S). A plane-wave kinetic energy cutoff of 550 eV was applied for the wavefunction, and a charge density cutoff of 2200 eV was used. Brillouin zone integration was performed using a 4×4×1 Monkhorst-Pack k-point grid. Geometry relaxation was carried out using the Broyden-Fletcher-Goldfarb-Shanno (BFGS) quasi-Newton algorithm with partial relaxation of the slab, allowing adsorbate atoms and the topmost surface layers to relax while keeping the bottom layers fixed. Surfaces were generated using ASE version 3.16.2 (fcc111 for Pt and hcp0001 for Ru, from ase.build) via the computational catalysis tool on NanoHub, with the (111) surface orientation, four surface layers, and a 10 Å vacuum layer separating periodic images (15, 16). The lateral cell parameters of the Ru(111) slab were a = 2.7719 Å, b = 2.7719 Å, as defined by the hexagonal cell vectors (2.771859, 0.000000, 0.000000), (1.385929, 2.400500, 0.000000), and (0.000000, 0.000000, 26.789639) in Ångstroms. The lateral cell parameters of the Pt(111) slab were a = 2.8225 Å, b = 2.8225 Å, as defined by the cell vectors (2.822500, 0.000000, 0.000000), (1.411250, 2.444000, 0.000000), and (0.000000, 0.000000, 26.900000) in Ångstroms.

Using Quantum ESPRESSO, simulations of surface adsorption on Pt and Ru surfaces were completed. Adsorption energy curves were generated by varying the adsorbate–surface distance across individual simulations. The distances from the surface that were used are (0.01, 0.1, 0.2, 0.3, 0.4, 0.5, 0.6, 0.7, 0.8, 0.9, 1, 1.5, 2, 2.5, 3, 3.5, 4, 4.5, 5, 5.5, and 6 Å). These distances were chosen to cover a range of potential chemisorption and physisorption binding modes. At closer distances (<1 Å), a finer resolution was used, while larger intervals were used at farther distances (> 1 Å). At each distance, the adsorption energy was measured, generating adsorption energy vs. distance curves. These adsorption energies were normalized by subtracting the average background, which was determined using the adsorption energy plateau at large distances (> 5 Å). The relative adsorption energy was computed as E_{axs} = E(slab+adsorbate) − E(slab) − E(molecule), normalized by subtracting the large-distance background; by this convention, more negative values indicate stronger adsorption. Replicate simulations (n=3) were repeated for select systems to determine simulation variability. The standard deviation of adsorption energy.

RESULTS

Figure 1 shows the adsorption energy curve for the Pt surfaces. The relative adsorption energy of NH_{33} is nearly always positive, indicating it exhibits no favorable chemisorption or physisorption interaction modes on the Pt surface. CO_2 displays broadly similar adsorption interactions with the exception of a very weak binding mode at 2.17 Å, with a relative interaction energy of 0.12 eV.

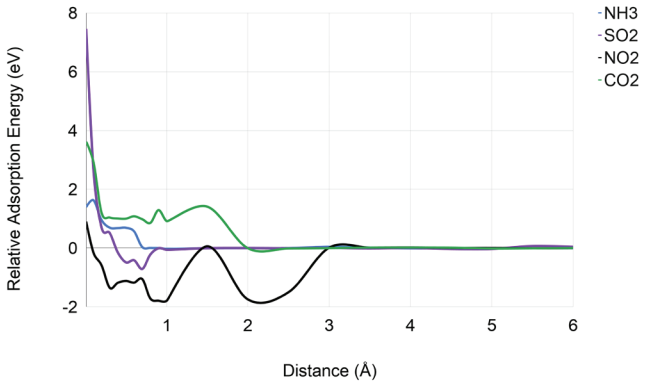

Figure 1. *Adsorption-energy versus initial adsorbate distance for NH_3, CO_2, SO_2, and NO_2 on the Pt (111) surface. The x-axis represents the initial adsorbate–surface distance (Å), and the y-axis represents the relative adsorption energy (eV). More negative values indicate stronger (more favorable) adsorption; values here are background-normalized (see Methods).*

In contrast, NO_2 and SO_2 exhibit more favorable interactions with the Pt surface. SO_2 shows a very weak bonding mode at 1 Å, with a relative energy of 0.05 eV and no activation barrier. Additionally, a closer chemisorption binding mode is observed at 0.70 Å (0.70 eV). NO_2 shows multiple favorable binding modes, exhibiting a physisorption binding mode at 2.15 Å, with an activation barrier of 0.12 eV and an interaction energy of 1.92 eV. A second relatively strong binding mode occurs at 1 Å, with an activation of 1.92 eV and an adsorption strength of 0.79 eV, likely indicating a chemisorption mode.

In Figure 2, the adsorption energy curve for Ru is shown. All adsorbates exhibit favorable chemisorption and/or physisorption binding modes. NH_3 shows a favorable binding mode at 0.46 Å with a relative interaction energy of 0.319 eV and an activation energy of 0.0110 eV. CO_2 exhibits similar behaviors to NH_3, with its most favorable binding mode occurring at 0.89 Å. This binding mode has an adsorption strength of 0.32 eV and an activation barrier of 0.0429 eV.

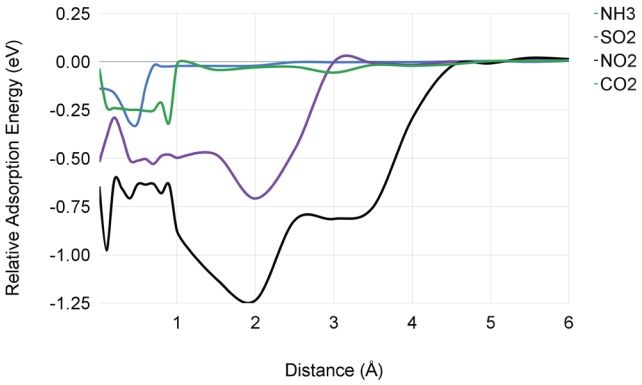

Figure 2. *Adsorption-energy versus initial adsorbate distance for NH_3, CO_2, SO_2, and NO_2 on the Ru (111) surface. The x-axis represents the initial adsorbate–surface distance (Å), and the y-axis represents the relative adsorption energy (eV).*

SO_2 and NO_2 also exhibit strong binding modes on the Ru surface. SO_2 displays its main binding mode at 2 Å with an adsorption strength of 0.739 eV and an activation barrier of 0.033 eV. Additional weaker binding modes are also present at >1 Å to the surface, with the strongest having a relative adsorption energy $_2$ exhibits two strong binding modes, the first at 3 Å with a relative adsorption energy of 0.814 eV and a negligible activation barrier, and the second at 1.9 Å with an adsorption strength of 1.248 eV (when compared with the baseline 0.459 eV above the activation energy) and an activation energy of 0.0245 eV. Additionally, weaker binding modes are present at >1 Å, with the strongest mode exhibiting a relative adsorption energy of 0.380 eV.

DISCUSSION

The results presented here highlight how many impurities in an ammonia stream may inhibit the progression of an ammonia decomposition reaction catalyzed by a Ru or Pt-based catalyst. All the contaminants tested exhibited significantly stronger binding modes at much farther distances than ammonia, as illustrated by Figure 3.

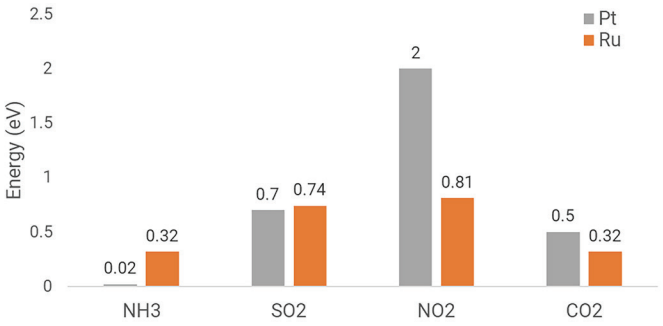

Figure 3. *Comparison of the strongest adsorption energies for each adsorbate on Pt and Ru surfaces. Comparison points correspond to the maximum relative adsorption energy magnitude observed for each adsorbate, consistent with the sign convention in Figures 1 and 2.*

The results here are consistent with previous studies which have demonstrated the vulnerability of Ru catalysts to sulfur-containing species. Hansen *et al*. emphasized the importance of gas purity for catalytic ammonia processes, while Larghi *et al*. reported strong sulfur poisoning of Ru catalysts during CO_2 methanation. Although the simulations examine ammonia decomposition rather than methanation, the stronger adsorption energies observed for SO_2 support the conclusion that sulfur-containing contaminants poison Ru active sites with relative frequency. Likewise, the NO_2 adsorption values suggest that nitrogen oxides may also outcompete NH_3 for adsorption sites, whereas CO_2 exhibits comparable adsorption values to NH_3 and therefore is predicted to present a substantially lower poisoning risk under ideal conditions.

As expected, Pt was highly unsuited for catalyzing an ammonia decomposition reaction. At the distance where ammonia interacted with the Pt surface, the adsorption energy was positive and, therefore, adsorption was unfavorable. The instability of this adsorption indicates that a high temperature would be needed for ammonia to bind to the surface involved. This has been previously reported and accounted for,(17) but it means that all contaminants would also be under high temperature if a Pt catalyst was used for ammonia decomposition.

On the same Pt surface, NO_2 and SO_2 adsorbates exhibit far more favorable binding modes when compared to ammonia. Both adsorbates exhibit stronger binding at distances farther than NH_3 and CO_2. CO_2, conversely, exhibited similar binding modes to ammonia. The primary difference consists of a marginally increased interaction distance along with a slightly higher relative adsorption energy. This indicates that poisoning from CO_2 contaminants is not likely in this scenario.

In contrast to the Pt surface, Ru provides a more suitable environment for adsorption. In this case, ammonia possesses favorable binding modes. These binding modes occur at 0.46 Å with an adsorption strength of 0.319 eV. Ammonia can, therefore, adsorb onto the Ru surface readily. Similarly, CO_2 displays binding modes that are highly comparable to ammonia, although CO_2 does possess a marginally stronger bond at a slightly farther point. CO_2's strongest and most significant binding mode occurs at 0.89 Å, with a relative adsorption energy of 0.32 eV. Furthermore, the shapes of the curves in both instances were similar. As such, CO_2 is of relatively little concern in regard to catalyst poisoning.

Like with the Pt surface, the SO_2 and NO_2 adsorbates are of much greater concern. Both adsorbates experience their binding modes at much farther distances, and both exhibit high relative adsorption energies. Both adsorbates form their strongest binding modes at around 2 Å with bond strengths of 0.739 and 1.248 eV, respectively. The high bonding distances coupled with the high adsorption energies indicate that active sites on the catalyst surface would be taken up prematurely by these adsorbates. In addition, the curves of the graphs are much steeper, meaning that more energy is required per unit of distance to break or alter the bonds of the adsorbates. All of these factors combined lead to SO_2 and NO_2 being highly disruptive contaminants, which may competitively poison catalyst surfaces under these modeled conditions and reduce reaction efficiency greatly.

Overall, the results support the original hypothesis. Ru exhibited lower vulnerability to NO_2 poisoning than Pt while remaining vulnerable to both SO_2 and NO_2 adsorption. In contrast, CO_2 displayed adsorption behavior comparable to NH_3 on the Ru surface, indicating that it is unlikely to act as a major contaminant under the conditions modeled.

CONCLUSION

Overall, of the contaminants that could be found in an industrial ammonia stream, results suggest that SO_2 and NO_2 are likely to poison a catalyst in an ammonia decomposition reaction. Ru catalysts in particular, which are one of the most common catalysts for ammonia decomposition,(5) are highly vulnerable to poisoning by SO_2 and NO_2 adsorbates. However, it should be noted that compared to Pt, Ru has far more favorable binding

modes for ammonia decomposition reactions. On a Ru surface, NH_3 goes from having all unstable binding sites to having a stable binding site with favorable binding energies. Additionally, both NO_2 and SO_2 have significantly less stable binding modes on a Ru surface as compared to a Pt one.

As such, it is recommended that future studies evaluate whether modified Ru-based catalysts can reduce contaminant adsorption while maintaining favorable NH_3 adsorption characteristics. Despite this, great care must still be taken to purify ammonia streams of SO_2 or NO_2 before being used to store hydrogen through NH_3 decomposition. Despite Pt's strong binding modes, results suggest that Pt-containing materials may warrant future investigation as sacrificial adsorption layers or contaminant filters; however, studies are required before further conclusions can be drawn.

CONFLICT OF INTEREST

The author declares no conflicts of interest related to this work.

REFERENCES

1. Singh S, Jain S, Ps V, Tiwari AK, Nouni MR, Pandey JK, *et al*. Hydrogen: A sustainable fuel for future of the transport sector. *Renew Sustain Energy Rev*. 2015 Nov; 51: 623–33. doi:10.1016/j.rser.2015.06.040
2. Fayaz H, Saidur R, Razali N, Anuar FS, Saleman AR, Islam MR. An overview of hydrogen as a vehicle fuel. *Renew Sustain Energy Rev.* 2012 Oct; 16 (8): 5511–28. doi:10.1016/j.rser.2012.06.012
3. Contreras A, Yiğit S, Özay K, Veziroğlu TN. Hydrogen as aviation fuel: A comparison with hydrocarbon fuels. *Int J Hydrog Energy*. 1997 Oct 1; 22 (10): 1053–60. doi:10.1016/S0360-3199(97)00008-6
4. Kojima Y, Yamaguchi M. Ammonia as a hydrogen energy carrier. *Int J Hydrog Energy.* 2022 Jun; 47 (54): 22832–9. doi:10.1016/j.ijhydene.2022.05.096
5. Sun S, Jiang Q, Zhao D, Cao T, Sha H, Zhang C, *et al*. Ammonia as hydrogen carrier: Advances in ammonia decomposition catalysts for promising hydrogen production. *Renew Sustain Energy Rev.* 2022 Nov 1; 169: 112918. doi:10.1016/j.rser.2022.112918
6. Wang Q, Zhou H, Pan S, Cui D, Bai J, Wu S, *et al*. Current research, reaction mechanisms, and future prospects of Ru-based catalysts and bimetallic catalysts for ammonia decomposition. *J Energy Inst*. 2025 Dec 1; 123: 102299. doi:10.1016/j.joei.2025.102299
7. Hansen SI, Sjølin BH, Castelli IE, Vegge T, Jensen AD, Christensen JM. The importance of gas purity in catalytic ammonia synthesis. *J Catal.* 2025 Oct; 450: 116223. doi:10.1016/j.jcat.2025.116223
8. Folke J, Song H, Schittkowski J, Schlögl R, Ruland H. Oxygen Poisoning in Laboratory Testing of Iron-Based Ammonia Synthesis Catalysts and its Potential Sources. *Chem Ing Tech*. 2020; 92 (10): 1372–8. doi:10.1002/cite.202000100
9. Palmisano V, Weidner E, Boon-Brett L, Bonato C, Harskamp F, Moretto P, *et al*. Selectivity and resistance to poisons of commercial hydrogen sensors. *Int J Hydrog Energy*. 2015 Sep; 40 (35): 11740–7. doi:10.1016/j.ijhydene.2015.02.120
10. Larghi C, Porta A, Etzi M, Fiori G, Visconti CG, Szanyi J, *et al*. Reactivity and characterization of S-poisoning on Ru/Al2O3 catalysts for CO_2 methanation. *Appl Catal B Environ Energy*. 2026 May 15; 385: 126336. doi:10.1016/j.apcatb.2025.126336
11. Giannozzi P, Baroni S, Bonini N, Calandra M, Car R, Cavazzoni C, *et al*. QUANTUM ESPRESSO: a modular and open-source software project for quantum simulations of materials. *J Phys Condens Matter.* 2009; 21 (39): 395502. doi:10.1088/0953-8984/21/39/395502
12. Giannozzi P, Andreussi O, Brumme T, Bunau O, Buongiorno Nardelli M, Calandra M, *et al*. Advanced capabilities for materials modelling with Quantum ESPRESSO. *J Phys Condens Matter.* 2017; 29 (46): 465901. doi:10.1088/1361-648X/aa8f79
13. Baseden KA, Tye JW. Introduction to Density Functional Theory: Calculations by Hand on the Helium Atom. *J Chem Educ*. 2014 Dec 9; 91 (12): 2116–23. doi:10.1021/ed5004788
14. Li H, Mo A, Li W, Ma X, Xiong Y, Shao P, *et al*. First-principles study on the adsorption, binding, and aggregation behaviors of W, B, C, O, and H atoms on the Mo(110) surface. *Nucl Mater Energy*. 2026 Sep; 48: 102178. doi:10.1016/j.nme.2026.102178
15. Hjorth Larsen A, Jørgen Mortensen J, Blomqvist J, Castelli IE, Christensen R, Dułak M, *et al*. The atomic simulation environment-a Python library for working with atoms. *J Phys Condens Matter Inst Phys J*. 2017 Jul 12; 29 (27): 273002. doi:10.1088/1361-648X/aa680e PubMed PMID: 28323250.
16. Sun W, Ceder G. Efficient creation and convergence of surface slabs. *Surf Sci*. 2013 Nov; 617: 53–9. doi:10.1016/j.susc.2013.05.016
17. Han T, Wei L, Xie S, Liu Y, Dai H, Deng J. Catalyst design for ammonia decomposition: an overview. *Ind Chem Mater.* 2025; 3 (3): 311–31. doi:10.1039/D4IM00112E